

Theoretical Study of the O₂ + Al₄ (Tetrahedral) System in Its Singlet State and Comparisons with Its Triplet State

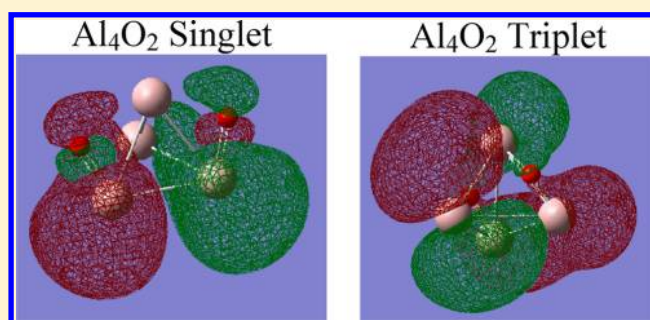
Naoum C. Bacalis* and Aristophanes Metropoulos

Institute of Theoretical and Physical Chemistry, National Hellenic Research Foundation, 48 Vass. Constantinou Avenue, Athens 11635, Greece

Axel Gross

Institute of Theoretical Chemistry, Ulm University, D-89069 Ulm, Germany

ABSTRACT: There is an unresolved discrepancy between theory and experiment about the observed hindrance in dissociative adsorption of O₂ on Al(111). In an attempt to understand the hindrance, we have investigated the interaction of O₂ with a tetrahedral Al₄ cluster (the apex considered as adatom) in a total singlet state by employing both the multireference configuration interaction (MRCI) and the density functional theory (DFT) methods. For an approach of O₂ facing an apex of the Al₄ pyramid and parallel to its base, both the MRCI and the DFT calculations show that after an early barrier the system goes through a narrow local minimum before it reaches a deep minimum of ~203 kcal/mol near the pyramid base. The O₂ molecule opens continuously, followed by a small decrease in the O–O distance around the deep minimum, forming antibonding orbitals with the pyramid base, whereas the O–O distance starts increasing in further increasing the incident energy. These results differ from previous results obtained for the same system but in a total triplet state, which showed two similar minima (one local narrow and one deep) but where O₂ is dissociatively adsorbed to the pyramid base, forming bonding orbitals with it. The reason for this difference is discussed. Total triplet is an excited state where the bound O–O becomes spinless and the spin density is transferred to the pyramid apex. Similar transfers occur on an Al₁₆ cluster formed by extending the pyramid base to a (111) arrangement. Our findings are contrasted with known results about the interaction of O₂ with Si clusters. The effect of the spin state on the interaction of O₂ with the planar Al base suggests that spin should be considered in an analysis of O₂ adsorption on aluminum surfaces as well. To our understanding, to increase the sticking probability, free O₂ must be, before incidence, prepared in *singlet*.



INTRODUCTION

This work is a continuation of our effort to understand a discrepancy between computation and experiment regarding the adsorption hindrance during dissociative adsorption of O₂ on Al(111), attributed to a small barrier, as indicated by molecular beam results.^{1,2} There have been various attempts to describe this hindrance theoretically because standard electronically adiabatic periodic DFT calculations have found that the dissociation of O₂ on Al(111) is not hindered by any barrier; that is, the adsorption should occur spontaneously,^{3–6} in contrast with the experiment. It has been suggested that the low sticking probability for thermal O₂ molecules impinging on Al(111) could be explained by assuming diabatic approach of O₂ in its gas-phase triplet state without adiabatically switching to a singlet state near the surface.^{7–11} This explanation has been supported by the observation of spin-selection rules in the interaction of O₂ with small Al anion clusters (~10 to 20 atoms) leading to odd/even pattern in the reactivity with O₂ as a function of the number *n* of atoms in the Al clusters.¹² The

present calculations, in the presence of an adatom, also support this suggestion.

The importance of interactions of oxygen with metal surfaces for heterogeneous catalysis has been discussed in two recent papers^{13,14} where the reactivity of O₂ (³Σ_g⁻) with planar and tetrahedral Al₄ clusters was investigated at both the multireference configuration interaction (MRCI) and the density functional theory (DFT) levels. The comparisons of DFT with accurate MRCI calculations were motivated by the question about the existence of an activation barrier in the adsorption of O₂ on Al crystal, related to the dissociative adsorption hindrance; and the motivation for the choice of a tetrahedral geometry was to approximate the outcome of a possible collision of oxygen with defect sites of Al such as adatoms. A comparison of DFT results with MRCI can be accomplished only in systems of small Al clusters where MRCI calculations

Received: February 14, 2012

Revised: June 15, 2012

can be applied, hoping that the conclusions can serve as a clue concerning the role of adatom surface crystal defects. Of course, the calculations are not only helpful for the understanding of the interaction of O₂ with Al defect sites but should also be relevant as far as the adsorption of O₂ on small Al clusters is concerned.

The DFT results in ref 13 showed a lack of any barrier, and it was suspected that this could be an artifact of the improper description of many-body effects in the employed GGA functional. However, cluster calculations within a richer basis-set, using a hybrid DFT functional with a certain fraction of Fock exchange, found a nonvanishing barrier in the O₂ adsorption on top of an Al adatom.¹⁴ These results indicate that apart from the basis functions, exchange-correlation effects are crucial for the determination of the adsorption barrier in the system O₂/Al. A partial list of important theoretical and experimental work on O₂/surface and on the O₂/Al_n systems is listed in refs 13 and 14.

In ref 14, the interaction of O₂ with a tetrahedral Al₄ cluster in a triplet total spin was explored. The main results from ref 14 were that for an approach of O₂ facing an apex of the pyramid, in a triplet total spin, both the MRCI and the DFT calculations showed that after a small barrier there was a narrow local minimum just above the apex atom at ~80 kcal/mol. Deeper below the apex atom there was an energy minimum at ~200 kcal/mol. The latter corresponds to the dissociative adsorption of O₂. The former traps O₂ on top of the apex until O₂ overcomes a barrier of ~10 kcal/mol toward full dissociative adsorption at ~120 kcal/mol below the trap. Such a trap still exists when the base of the Al₄ pyramid is expanded from 3 to 15 Al atoms, simulating a larger part of the Al(111) surface. For these calculations, improved basis functions were used, and we found a larger barrier in MRCI calculations than in DFT calculations. Nevertheless, these energy values mean that an Al adatom is not necessarily more active toward O₂ dissociation than Al atoms in a planar geometry. They also mean that the vanishing barrier for the O₂ adsorption on Al(111) found in periodic DFT calculations might still be an artifact of the employed functionals (rather than the basis functions); such periodic DFT calculations were performed electronically adiabatically in a spin-nonpolarized fashion, that is, in a singlet state for both the O₂ and the Al(111) surface, and yielded a purely attractive path for O₂ adsorption.^{9,11} Thus, the problem of the theoretical description of the hindrance remained.

In the present work, we explore the interaction of O₂ with a tetrahedral Al₄ cluster in a singlet rather than triplet total spin. The reasoning for the choice of a tetrahedral cluster is the same as the one advanced in the triplet spin case of the previous paragraphs.¹⁴ As explained in ref 14, approaches under other angles, that is, the largest part of phase space, are intricate and complex, involving pronounced orientation dependence. These would open up possibilities for molecular precursors and abstraction via intermediate molecularly chemisorbed states.⁵ A complete study of the potential energy surface (PES) is beyond the scope of this article, much less because in a vertical O₂ approach MRCI presented technical problems, for example, convergence, rendering its success doubtful, and the present DFT potentials might give doubtful results as well. To check the trends, after examining the similarities and the differences between the total singlet (present work) and total triplet¹⁴ cases, we extended the study of the important features to a larger Al₁₆ cluster, simulating a more extended Al(111) surface with an Al adatom on it. The preservation of the features, as

reported below, indicates that the triplet spin may be the determining factor in understanding the puzzling hindrance.^{7–11}

Preliminary Considerations. It is known that the optimal geometry of the cluster is the planar one,¹³ and that the rhombus geometry has the lowest energy.¹⁴ The relative energies of the basic Al₄ structures are shown in figure 1 and table 1 of ref 14. The tetrahedral structure is ~10 kcal/mol above the ground state of rhombus. We set up the Al₄ cluster in a tetrahedral geometry so that all angles between the sides are 60° and all sides have a length of 2.7 Å. We selected one apex of the pyramid as a reference point, say Al1, and this defined a reference base of the pyramid as the base opposite to Al1. The Al atoms at this base were denoted by Al2, Al3, and Al4. We defined Al1 as the origin of the coordinate system with the *z* axis vertical to the base and the *y* axis parallel to the Al3–Al4 side of the base. An oxygen molecule was added along the *z* axis so that the O–O center of mass lied on this axis and the O–O line was permanently parallel to the *y* axis. The Al2 atom was on a line parallel to the *x* axis. The distance of the O–O center of mass from the origin Al1 is denoted by *Z*, and the O–O separation is denoted by *r*.

Details of the Calculation. We started both the MRCI and the DFT calculations at *Z* = 5 Å and *r* = 1.20 Å and proceeded at smaller and smaller *Z* values. At each *Z* only the O–O separation, *r*, was optimized by running calculations at intervals of Δ*r* = 0.05 Å for CI and at Δ*r* = 0.02 Å for DFT. The overall system was taken to be a singlet so that the interaction might, in principle, be considered between either a singlet Al₄ (excited state) with a singlet O₂ (lowest excited state) or as a quintet Al₄ (ground state, almost degenerate with the lowest excited triplet, not reported in ref 14) with a triplet O₂ (ground state). Therefore, because the Al(111) extended substrate (simulated here by the Al₄ or the Al₁₆ cluster) corresponds to a singlet state, relevant electronic structure details, implicitly suggested in refs 7–11 are expected to show up in total singlet, to be compared with total triplet.

For the MRCI calculations, we employed the MOLPRO package¹⁵ with the cc-pVTZ basis set of Dunning et al.¹⁶ The calculations on the Al₄ + O₂ system were done in C₁ symmetry so that at the SCF level all 68 electrons were distributed in 34 orbitals of the single symmetry of C₁, all of them doubly occupied. We generated a reduced active space (RAS) by distributing the 20 valence electrons in 12 orbitals (20/12) at the MCSCF step. All MRCI calculations were run using these MCSCF/RAS orbitals.

For the DFT calculations, we employed the GAUSSIAN-03 package¹⁷ using the split-valence triple-ζ basis set 6-311+g* with polarization and diffuse functions^{18–20} and the Becke three-parameter (exchange), Lee, Yang, and Parr (correlation) density functional (B3LYP).^{21–24} All 68 electrons are in 34 Kohn–Sham orbitals of C₁ symmetry. However, surprisingly, the 6-311+g* basis set yielded *unreasonably positively* charged O atoms below the apex; therefore, we recomputed several important points using the correlation-consistent polarized valence quadruple-ζ (cc-pVQZ) basis set,¹⁶ which showed reasonable charges (checked also by full-CI cc-pVQZ calculations at the energy minimum). Nevertheless, the two basis sets yielded *equivalent energies* (cf. Figure 1). Except for the DFT 6-311+g* full curve of Figure 1, which was verified by cc-pVQZ at some important points, all other important results in Table 1 and Figure 2 have been recalculated using the cc-

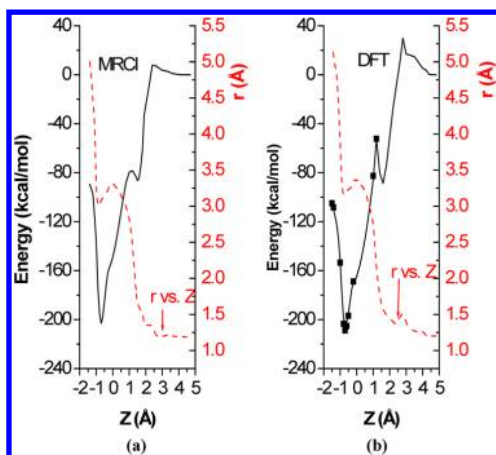


Figure 1. PES cut (black) and O–O distance, r , (red) as functions of the Al1–O₂ distance, Z , calculated (a) by the MOLPRO/CI method and (b) by the DFT method for a total singlet state. In panel b, the solid line has been computed by using the 6-311+g* basis, and the dot points have been computed by using the cc-pVQZ basis. Both basis sets give the same energies, but 6-311+g* gives unreasonable Mulliken charges (positive) on O atoms, whereas cc-pVQZ gives reasonable charges. The main difference from ref 14 (triplet) is that in approaching the pyramid base for $Z < -1$ Å the O–O distance in singlet increases, whereas in triplet¹⁴ it decreased.

pVQZ basis set. For the larger cluster of Al₁₆O₂, SCF with cc-pVQZ was used.

RESULTS AND DISCUSSION

The calculated PESs cut for MRCI and DFT are shown in Figure 1a,b, respectively along with the O–O distance, r , as a

function of Z . Both methods give similar results: For MRCI, there is an activation barrier of ~ 8 kcal/mol at $Z \approx 2.4$ Å and $r \approx 1.35$ Å, a narrow local minimum at $Z \approx 1.5$ Å and $r \approx 1.65$ Å, and a deep minimum of ~ 203 kcal/mol at $Z \approx -0.7$ Å and $r \approx 3.1$ Å. For DFT, the activation barrier is 30 kcal/mol at $Z \approx 2.8$ Å and $r \approx 1.55$ Å, the narrow local minimum is at $Z \approx 1.60$ Å and $r \approx 1.56$ Å, and the deep minimum is ~ 205 kcal/mol at $Z \approx -0.7$ Å and $r \approx 3.16$ Å. In both methods, we observe that the O–O bond opens from 1.2 to 3.3 Å as the oxygen approaches the apex of the pyramid ($Z = 0$) and then diminishes slightly to 3.2 Å near the minimum ($Z \approx -0.7$ Å). For $Z < -0.7$ Å, corresponding to larger incident energies, the energy increases again and r decreases a little more to 3.1 Å. Up to this point, the behavior of the singlet is very similar to that of the triplet, as seen from the corresponding figure of ref 14 but at lower Z , achieved at higher incident energies, there appears a difference: In triplet (ref 14) r decreases to 2 Å,¹⁴ forming bonding Al–O orbitals, as presented below. Contrary to the triplet, here in the singlet, r increases to ~ 5 Å at $Z = -1.4$ Å, where the calculation stopped, forming antibonding Al–O orbitals with the pyramid base.

In investigating the reason for these differences in behavior, as revealed by both the MRCI and the DFT methods, we examined, in cc-pVQZ DFT, the HOMO Kohn–Sham orbitals (cf. Figure 2) of both singlet and triplet states. This was done for both cases at the optimized O–O distances $r = 2.6$ Å (optimized at $Z = -1$ Å in the triplet case) and $r = 3.8$ Å (optimized at $Z = -1.15$ Å in the singlet case). These Z values were chosen based on a better visibility of these (r, Z) points in the r versus Z curves of Figure 1b and of the corresponding figure of ref 14.

Table 1. MRCI and DFT cc-pVQZ Charge Transfer through Mulliken Population Analysis^a

	Z	r	Al1	Al2	Al3+Al4	O1+O2	HOMO–LUMO gap (E_h)
Singlet Al ₄ O ₂							
DFT	–0.80	3.20	+0.45	+0.10	+0.32	–0.88	0.07
	–1.00	3.80	+0.40	+0.20	+0.26	–0.86	0.07
MRCI	–0.80	3.20	+0.70	+0.04	+0.57	–1.31	
	–1.00	3.80	+0.40	+0.24	+0.60	–1.24	
	–1.15	2.60	+0.42	+0.20	+0.72	–1.34	
Singlet Al ₁₆ O ₂							
SCF	–1.15	2.60	+0.30	–0.23	+0.78	–1.36	0.16
	–1.00	3.80	+0.31	–0.38	+0.54	–1.36	0.12
Triplet Al ₄ O ₂							
DFT	–0.80	3.20	+0.50	+0.04	+0.33	–0.88	0.07/0.07
			+0.90	+0.54	+0.46	+0.12	
	–1.15	2.60	+0.48	+0.00	+0.26	–0.74	0.07/0.03
			+1.08	+0.57	+0.26	+0.12	
MRCI	–0.80	3.20	+0.72	+0.04	+0.55	–1.32	
	–1.00	3.80	+0.50	+0.12	+0.62	–1.23	
	–1.15	2.60	+0.71	+0.05	+0.71	–1.37	
Triplet Al ₁₆ O ₂							
SCF	–1.15	2.60	+0.26	–0.28	+0.82	–1.36	0.18/0.16
			–0.03	–0.13	–0.16	+0.03	
	–1.00	3.80	+0.37	–0.28	+0.56	–1.36	0.17/0.17
			–0.30	–0.07	–0.20	–0.02	

^aAll1 is at the apex of the pyramid, Al2 is vertical to the projection of the O–O axis on the base of the pyramid, whereas Al3 and Al4 are parallel to the O–O axis, \pm signify positive/negative charges. Distances are in angstroms. $Z = -0.8$ Å is the energy minimum, and the other positions $Z = -1.0$ Å and -1.15 Å are beyond equilibrium, where the O atoms have been separated. For the triplet HOMO/LUMO gap, in E_h , the two numbers correspond to “majority-/minority-spin”. In triplet, each second row shows the Mulliken spin density. For the large clusters, Al₁₆O₂ SCF values are given.

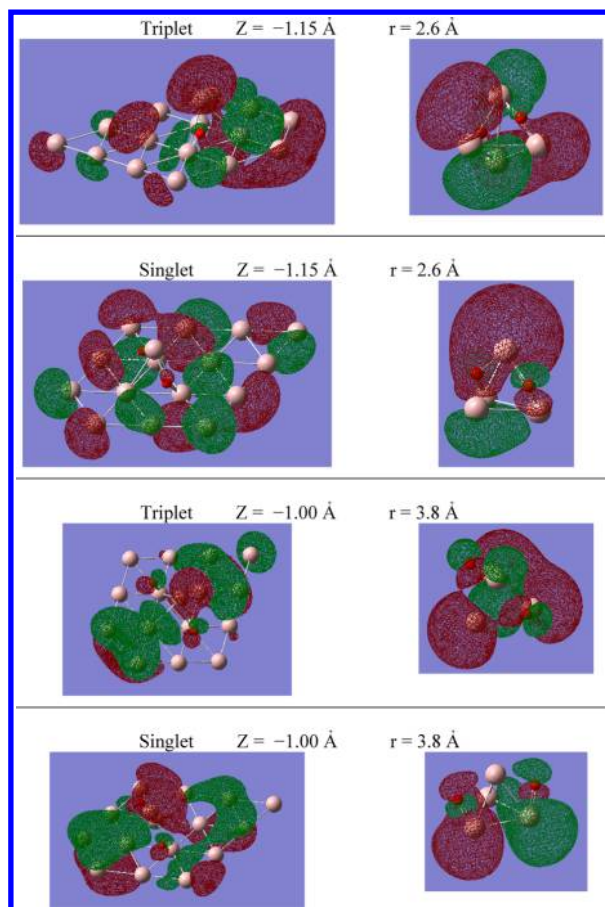


Figure 2. HOMO orbital, using cc-pVQZ basis set, of total spin triplet and singlet at O_2 (r , Z) coordinates (2.6, -1.15) and (3.8, -1.00) in angstroms, interacting with Al_{16} cluster (left panels, SCF orbital) and Al_4 cluster (right panels, Kohn–Sham orbital). These coordinates were chosen well beyond the potential energy minimum of Figure 1 or of the corresponding figure for the triplet (cf. ref 14). At these geometries, the orbitals show that the dissociated O–O binds to the Al cluster only in total spin triplet state (the upper panel in which triplet is optimized). In all other panels (either singlet in optimized triplet’s position, or optimized singlet, or triplet in optimized singlet’s position), the HOMO orbitals are antibonding.

As seen in the upper panel of Figure 2, (triplet at $Z = -1.15$ Å, optimum for triplet $r = 2.6$ Å), each O atom (red) forms a *bonding* HOMO orbital with mainly its neighboring “surface” Al atom (beige) in both the Al_4 (right) and Al_{16} clusters (left). However, for the singlet at the same geometry (second panel of Figure 2), as it is evident from the nodal surfaces between the atoms, the corresponding HOMO orbital is *antibonding* in both the Al_4 (right) and Al_{16} clusters (left). Also antibonding are the HOMO orbitals in both singlet (at $Z = -1$ Å, optimum for singlet $r = 3.8$ Å) and triplet at the same geometry, as seen in the two lower panels of Figure 2. (In singlet, at these positions, the first lower bonding orbital, $0.1 E_h$ deeper than HOMO, is HOMO-3). Therefore, the HOMO orbital is antibonding in all cases except in the majority-spin *triplet*, in which the separated O atoms form a *bonding* orbital binding mainly to the closest Al atoms of the lower pyramid *base*. To ascertain whether this behavior could be maintained around an Al(111) surface adatom, we expanded the pyramid base by adding 12 Al atoms in such a manner as to obtain a portion of an Al(111) surface consisting of 15 Al atoms: Indeed (cf. left panels of Figure 2), the HOMO orbital is antibonding in all cases (singlet and

triplet) except in the minority-spin triplet, in which the separated O atoms (at the same (r , Z) values as in the “pyramid” case) form a bonding HOMO orbital binding to only the “surface” atoms. Therefore, below the Al adatom, O_2 dissociates adsorbed to the *surface* Al atoms in the total spin triplet state, but it dissociates without binding to the surface Al atoms in the total spin singlet state, forming antibonding HOMO orbitals at both Al_4 and Al_{16} structures (cf. Figure 2).

To examine the charge transfer during the examined processes, we computed the Mulliken charge and spin distributions in the above cases. By using the 6-311+g* basis set at the above nonequilibrium positions, the O atoms in forming antibonding orbitals with the pyramid basis (“surface”) showed to be slightly *positively* charged, which was intuitively unexpected. To investigate the unexpected positive charge on oxygen, we repeated the same calculations in all important positions, using RAS configuration interaction (MRCI) with 20 electrons in 12 orbitals and cc-pVQZ basis. The Mulliken charges now were reasonable, so we believe that the cc-pVQZ calculations are more reliable than those of 6-311+g*, although the energy trends are similar. For this reason, we recalculated all important points by cc-pVQZ DFT. Table 1 shows the charge distributions on the atoms and the Mulliken spin density (in the triplet case) as well as the HOMO–LUMO gaps at the above geometries and at the lowest energy minimum of Al_4O_2 . From this Table, it is evident that for the *singlet* case at the minimum of Al_4O_2 ($Z \approx -0.8$ Å, $r \approx 3.2$ Å) there is some electron transfer from the pyramid side close to O–O (Al1–Al3–Al4). The Al3 and Al4 atoms are bound to the O atoms. Deeper, beyond the local minimum of the O–O separation, needing high incident energy, at $Z = -1.00$ Å, $r = 3.8$ Å (i.e., optimized r for the singlet), some electron charge leaves the pyramid basis (Al2–Al3–Al4). In $Al_{16}O_2$, at same positions as in the pyramid there is a similar behavior showing some electron transfer from the base of the pyramid.

The same Table shows that for the *triplet* Al_4O_2 , at the minimum ($Z \approx -0.8$ Å, $r \approx 3.2$ Å), O–O binds at the same place as in singlet, but the apex Al1 seems to be slightly more reactive than in singlet. The total spin (2.0) is distributed as shown in Table 1. Contrary to free space O_2 , O–O is not in triplet any more, indicating that a spin exchange between oxygen and the cluster is needed. Deeper (for higher incident energies), again beyond the local O–O minimum separation, at $Z = -1.15$ Å, $r = 2.6$ Å (i.e., optimized r for the triplet), we have a similar transfer. The O atoms are bound to Al3 and Al4, whereas the opposite Al2 remains inactive. The total *spin* as shown in Table 1 is still distributed mainly around the apex Al1, the opposite Al2, and to each of the O neighbors Al3, Al4, whereas O–O is essentially in singlet. Similarly, in $Al_{16}O_2$, there is also some electron transfer from the base of the pyramid. The O atoms are bound to the neighbors Al3, Al4 by minority-spin. The total *spin* is distributed mainly around the apex Al1 and slightly in other Al atoms, whereas the dissociated O–O is clearly in singlet. In the Al_4 – O_2 dissociation limit, O_2 is in triplet (${}^3QCISD^{25} = -150.220E_h$) and Al_4 is in quintet (${}^5QCISD = -968.065E_h$), almost degenerate with triplet (${}^3QCISD = -968.062E_h$), whereas O_2 in singlet has energy ${}^1QCISD = -150.168E_h$ and Al_4 has ${}^4QCISD = -968.058E_h$. Therefore, in incoming, the ground state of the separated system is triplet ($-1118.285E_h$), slightly lower than the singlet ($-1118.282E_h$). Therefore, there is an adiabatic spin exchange when they interact as described above.

We also observed an energy reversal between CI and SCF (and DFT) and between singlet and triplet: At SCF level (and DFT), the ground state at equilibrium is triplet, whereas at CI level it is *singlet*. For the absolute minimum (m) ($Z = -0.8 \text{ \AA}$), as well as at the “triplet trend (tt)” ($\text{O}-\text{O}$ distance $r = 2.6 \text{ \AA}$), at SCF level, the triplet (${}^3\text{SCF}_m = -1117.55E_h$ and ${}^3\text{SCF}_{tt} = -1117.260E_h$) (the upper prefix indicates the spin multiplicity) is lower than the singlet (${}^1\text{SCF}_m = -1117.52 E_h$ and ${}^1\text{SCF}_{tt} = -1117.256E_h$), whereas at CI level, as well as full-CI at the absolute minimum, the singlet (${}^1\text{MRCI}_m = -1118.221E_h$, ${}^1\text{Full-CI}_m = -1118.640E_h$, and ${}^1\text{MRCI}_{tt} = -1117.891E_h$), is lower than the triplet (${}^3\text{MRCI}_m = -1118.207E_h$, ${}^3\text{Full-CI}_m = -1118.630E_h$, and ${}^3\text{MRCI}_{tt} = -1117.849E_h$). This is also in contradiction with the DFT results. At the “singlet trend (st)” ($r = 3.8 \text{ \AA}$), no energy reversal occurs between SCF (${}^1\text{SCF}_{st} = 1117.44 E_h$, ${}^3\text{SCF}_{st} = -1117.42 E_h$) and CI (${}^1\text{MRCI}_{st} = -1118.133E_h$, ${}^3\text{MRCI}_{st} = -1118.074E_h$). It is clear that at equilibrium singlet is the ground state but forms an antibonding HOMO orbital, whereas triplet, which forms bonding HOMO orbital, is an excited state. Evidently the subject would need further investigation at the CI level.

It is interesting to contrast our findings with the results obtained for the interaction of O_2 with silicon clusters, which has been intensively studied^{26–28} due to the importance of the O_2 –Si interaction in manufacturing of semiconductor devices. Of course Si as a semiconductor has a rather different electronic structure than the metal Al. Still, DFT calculations of the interaction of O_2 with neutral Si clusters found that the dissociation of O_2 on Si_4 is hindered by a barrier of ~ 10 kcal/mol.²⁹ In another study, using the full potential linear muffintin orbital (FP-LMTO) molecular dynamics method, this barrier was estimated to be ~ 19 kcal/mol.³⁰ Larger Si clusters showed, in general, a larger energy gain for O_2 dissociative adsorption than the Si_4 cluster. Still, the authors of this DFT study concluded that also for these larger, more reactive Si clusters a barrier toward dissociative adsorption should be overcome if spin conservation along the reaction path is considered.²⁹ For positively charged Si clusters, it was found that large clusters are ~ 100 times less reactive toward O_2 than most bulk silicon surfaces.³¹ Barriers have also been calculated in various stages of $\text{Al}(100) + \text{O}_2$ reactions.³²

CONCLUSIONS

We studied the behavior of O_2 as it approaches the apex of a tetrahedral Al_4 cluster in a total spin singlet state moving toward the base of the pyramid. A comparison with the behavior of the corresponding total spin triplet state was made. We also expanded the pyramid base by adding 12 more Al atoms around it in a surface $\text{Al}(111)$ arrangement, to check that the important electronic characteristics are maintained.

In both spin states, there is a low barrier above the apex Al1, a narrow local energy minimum just below the apex, and a binding minimum even deeper below the apex, where $\text{O}-\text{O}$ binds dissociatively. Below this, the energy increases differently: In triplet, the $\text{O}-\text{O}$ distance decreases, maintaining one bonding orbital of each O with Al atoms belonging to the pyramid base (HOMO), whereas, in singlet, the $\text{O}-\text{O}$ distance increases, forming all antibonding $\text{O}-\text{Al}$ orbitals that might lead to complete $\text{O}-\text{O}$ dissociation at higher collision energies.

Although $\text{O}-\text{O}$ binds essentially at the same place below the apex Al1 in both the singlet and triplet cases, the spin distributions differ significantly. As O_2 moves deeper toward the pyramid base, the O atoms attract electronic charge mainly

from the pyramid base, whereas simultaneously they tend to become spinless (singlet). This seems to be achieved by exchanging, through binding, their free-space stable “parallel spin” electrons (triplet in the free space O_2) with the Al cluster’s “antiparallel spin” electrons. This state has been obtained adiabatically. In other words, it seems that in triplet, while binding, the two “parallel” electrons of O_2 are exchanged adiabatically with two “antiparallel” electrons of the cluster. We do not expect that this state could be obtained by a quick diabatic process but rather $\text{O}-\text{O}$ would, diabatically, stay in triplet during collision. If this electron exchange is indeed unfavorable by quick diabatic processes during collision, then we believe that the inability for quick electron transfer, required for binding in triplet, might contribute to the observed dissociative adsorption hindrance. On the contrary, because the ground state of O_2 is triplet, the fact that in total singlet $\text{O}-\text{O}$ dissociates near an Al adatom via antibonding orbitals might, in principle, be thought to contribute to reducing the sticking probability. The fact that there is a barrier for O_2 dissociative adsorption at the apex of a Al_4 cluster both in total spin triplet and singlet state at the DFT hybrid functional and the MRCI level indicates that the presence of this barrier is not an artifact of a particular spin state. Hence the absence of any barrier in periodic DFT calculations for $\text{O}_2/\text{Al}(111)$ could be a consequence of the functional used in these calculations that did not contain any exact exchange. The barrier might also be a consequence of the special geometry with the dissociation occurring at a protruding Al atom. This has to be checked in more detail, although it has to be noted that typically protruding atoms exhibit a higher reactivity. Still, the significant differences in the energetics and the electronic structure between the total triplet and total singlet calculations confirm that the spin state plays an important role in the dissociative adsorption process of O_2 on aluminum clusters and should also not be neglected in an analysis of O_2 adsorption on aluminum surfaces. The ground state at equilibrium is singlet, and the lowest singlet is achieved by incoming free triplet O_2 to a free triplet cluster. Because at the binding total triplet the apex Al1 accumulates significant spin density (close to 1) leaving the base “surface” singlet, whereas $\text{O}-\text{O}$ is spinless (singlet) at equilibrium, we conclude that the binding occurs between a singlet surface and a singlet incoming O_2 , in agreement with spin nonpolarized DFT calculations.^{9–11} Therefore, to our understanding, the hindrance is rather not due to a potential barrier but due to the fact that in the *ground state (singlet)*, beyond equilibrium, the separated $\text{O}-\text{O}$ forms antibonding orbitals with the surface. For O_2 to stay bound (by bonding orbitals), it ought to undergo diabatically an excitation to singlet by spin flipping, which cannot occur spontaneously during collision; to increase the sticking probability, free O_2 must be *prepared* (excited) in singlet before incidence. Such cases would, in principle, require computations of excited states. We have elaborated a variational principle for excited states not demanding orthogonality to lower-lying states of the same symmetry type.³³

AUTHOR INFORMATION

Corresponding Author

*E-mail: nbacalis@eie.gr.

Notes

The authors declare no competing financial interest.

ACKNOWLEDGMENTS

This work was partially supported by the IKYDA program of the German Academic Exchange Service (DAAD) and the Greek State Scholarships Foundation (I.K.Y.). Partial support of this work through the Excellence in the Research Institutes program, supervised by the General Secretariat for Research and Technology/Ministry of Development, Greece (Phase I and II, Projects 64769 and 200501330081), is gratefully acknowledged. Furthermore, we thank Dr. Katrin Tonigold, Ulm University, for technical assistance.

REFERENCES

- (1) Brune, H.; Wintterlin, J.; Behm, R. J.; Ertl, G. *Phys. Rev. Lett.* **1992**, *68*, 624.
- (2) Osterlund, L.; Zoric, I.; Kasemo, B. *Phys. Rev. B* **1997**, *55*, 15452.
- (3) Sasaki, T.; Ohno, T. *Surf. Sci.* **1999**, *433*, 172.
- (4) Honkala, K.; Laasonen, K. *Phys. Rev. Lett.* **2000**, *84*, 705.
- (5) Y. Yourdshahyan, Y.; Razaznejad, B.; Lundqvist, B. I. *Phys. Rev. B* **2002**, *65*, 075416.
- (6) Zhukovskii, Yu. F.; Jacobs, P. W. M.; Causá, M. J. *Phys. Chem. Solids* **2003**, *64*, 1317.
- (7) Behler, J.; Delley, B.; Lorenz, S.; Reuter, K.; Scheffler, M. *Phys. Rev. Lett.* **2005**, *94*, 036104.
- (8) Behler, J.; Delley, B.; Reuter, K.; Scheffler, M. *Phys. Rev. B* **2007**, *75*, 115409.
- (9) Behler, J.; Reuter, K.; Scheffler, M. *Phys. Rev. B* **2008**, *77*, 115421.
- (10) Carbogno, C.; Behler, J.; Groß, A.; Reuter, K. *Phys. Rev. Lett.* **2008**, *101*, 096104.
- (11) Carbogno, C.; Behler, J.; Reuter, K.; Groß, A. *Phys. Rev. B* **2010**, *81*, 035410.
- (12) Burgert, R.; Schnöckel, H.; Grubisic, A.; Li, X.; Bowen, S. T. S. K. H.; Ganteför, G. F.; Kiran, B.; Jena, P. *Science* **2008**, *319*, 438.
- (13) Mosch, C.; Koukounas, C.; Bacalis, N.; Metropoulos, A.; Groß, A.; Mavridis, A. J. *Phys. Chem. C* **2008**, *112*, 6924.
- (14) Bacalis, N.; Metropoulos, A.; Groß, A. *J. Phys. Chem. A* **2010**, *114*, 11746.
- (15) MOLPRO is a package of programs written by Werner H. J.; Knowles P. J., with contributions from Almlöf, J.; Amos R. D.; et al.
- (16) (a) Dunning, T. H. *J. Chem. Phys.* **1989**, *90*, 1007. (b) Kendall, R. A.; Dunning, T. H.; Harrison, R. J. *J. Chem. Phys.* **1992**, *96*, 6769. (c) Woon, D. E.; Dunning, T. H. *J. Chem. Phys.* **1993**, *98*, 1358.
- (17) Frisch, M. J.; Trucks, G. W.; Schlegel, H. B.; Scuseria, G. E.; Robb, M. A.; Cheeseman, J. R.; Montgomery, J. A., Jr.; Vreven, T.; Kudin, K. N.; Burant, J. C.; Millam, J. M.; Iyengar, S. S.; Tomasi, J.; Barone, V.; Mennucci, B.; Cossi, M.; Scalmani, G.; Rega, N.; Petersson, G. A.; Nakatsuji, H.; Hada, M.; Ehara, M.; Toyota, K.; Fukuda, R.; Hasegawa, J.; Ishida, M.; Nakajima, T.; Honda, Y.; Kitao, O.; Nakai, H.; Klene, M.; Li, X.; Knox, J. E.; Hratchian, H. P.; Cross, J. B.; Adamo, C.; Jaramillo, J.; Gomperts, R.; Stratmann, R. E.; Yazyev, O.; Austin, A. J.; Cammi, R.; Pomelli, C.; Ochterski, J. W.; Ayala, P. Y.; Morokuma, K.; Voth, G. A.; Salvador, P.; Dannenberg, J. J.; Zakrzewski, V. G.; Dapprich, S.; Daniels, A. D.; Strain, M. C.; Farkas, O.; Malick, D. K.; Rabuck, A. D.; Raghavachari, K.; Foresman, J. B.; Ortiz, J. V.; Cui, Q.; Baboul, A. G.; Clifford, S.; Cioslowski, J.; Stefanov, B. B.; Liu, G.; Liashenko, A.; Piskorz, P.; Komaromi, I.; Martin, R. L.; Fox, D. J.; Keith, T.; Al-Laham, M. A.; Peng, C. Y.; Nanayakkara, A.; Challacombe, M.; Gill, P. M. W.; Johnson, B.; Chen, W.; Wong, M. W.; Gonzalez, C.; Pople, J. A. *Gaussian 03*, revision C.02; Gaussian, Inc.: Wallingford, CT, 2004.
- (18) McLean, A. D.; Chandler, G. S. *J. Chem. Phys.* **1980**, *72*, 5639.
- (19) Krishnan, R.; Binkley, J. S.; Seeger, R.; Pople, J. A. *J. Chem. Phys.* **1980**, *72*, 650.
- (20) Frisch, M. J.; Pople, J. A.; Binkley, J. S. *J. Chem. Phys.* **1984**, *80*, 3265.
- (21) Becke, A. D. *J. Chem. Phys.* **1993**, *98*, 1372.
- (22) Lee, C.; Yang, W.; Parr, R. *Phys. Rev. B* **1988**, *37*, 785.
- (23) Vosko, S. H.; Wilk, L.; Nusair, M. *Can. J. Phys.* **1980**, *58*, 1200.
- (24) Stephens, P. J.; Devlin, F. J.; Chabalowski, C. F.; Frisch, M. J. *J. Phys. Chem.* **1994**, *98*, 11623.
- (25) Pople, J. A.; HeadGordon, M.; Raghavachari, K. *J. Chem. Phys.* **1987**, *87*, 5968.
- (26) Bergeron, D. E.; Castleman, A. W. *J. Chem. Phys.* **2002**, *117*, 3219.
- (27) Lu, W. C.; Wang, C. Z.; Nguyen, V.; Schmidt, M. W.; Gordon, M. S.; Ho, K. M. *J. Phys. Chem. A* **2003**, *107*, 6936.
- (28) Zang, Q. J.; Su, Z. M.; Lu, W. C.; Wang, C. Z.; Ho, K. M. *J. Phys. Chem. A* **2006**, *110*, 8151.
- (29) Li, S. F.; Gong, X. G. *J. Chem. Phys.* **2005**, *122*, 174311.
- (30) Li, B. X.; Cao, P. L.; Ye, Z. Z.; Zhang, R. Q.; Lee, S. T. *J. Phys.: Condens. Matter* **2002**, *14*, 1273.
- (31) Jarrold, M. F.; Ray, U.; Creegan, K. M. *J. Chem. Phys.* **1990**, *93*, 224.
- (32) Widjaja, Y.; Musgrave, C. B. *J. Chem. Phys.* **2002**, *116*, 5774.
- (33) Bacalis, N. C.; Xiong, Z.; Karaoulanis, D. *J. Comput. Methods Sci. Eng.* **2008**, *8*, 277.